Transactions of the Korean Nuclear Society Spring Meeting
Jeju, Korea, May 8-10, 2024

A Study on Secondary Frequency Operation in APR1400 Using Mode-K+

Husam Khalefih, Yunseok Jeong, andYonghee Kim
Department of Nuclear and Quantum Engineering, Korea Advanced Institute of Science and Technology (KAIST)
291 Daehak-ro, Yuseong-gu, Daejeon, 34141, Republic of Korea
husam.khalefih@kaist.ac.kr, yongheekim@kaist.ac.kr

***Keywords**: Mode-K+, Load-Follow Operation, APR1400

1. Introduction

Due to the nature of power grid operations, there is always uncertainty between power demand and production. This uncertainty increases with the growing contribution of intermittent renewable sources [1]. As a result, nuclear power plants, which were originally designed for base load operation, are now required to adapt to various Load-Following Operation (LFO) schemes. For instance, Figure 1 illustrates the grid frequency changes in Europe over a specific period. To minimize frequency deviation from the targeted value (i.e., 50 Hz), nuclear power plants must be capable of adjusting their output power at different rates [2]. The first scenario is called primary frequency operation, where power variation needs to be executed quickly, within a matter of seconds. The second type of operation, which we will discuss here, is secondary frequency operation. In this mode, the power plant must be capable of adjusting its power by ± 5% of its rated power (P_r) within several seconds to a few minutes. In some European requirements, a maximum speed of 5%Pr/min is considered.

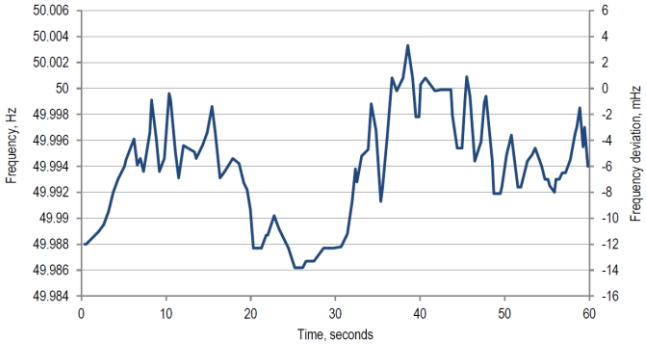

Figure 1 Typical example of Europe's electricity grid frequency for a period of time [1].

Various studies have examined the performance of Pressurized Water Reactors (PWRs) under frequency operation conditions. A. Abdelhameed et al. research focused on autonomous frequency operation in both conventional large-size PWRs and small-size soluble boron-free PWRs. Their study demonstrated that adjusting the inlet coolant temperature enables frequency operation without altering the control rod position. However, this capability is subject to limitations and varies based on the operational strategy and the size of the pressurizer used in the PWRs [3,4]. Additionally, Wang Pengfei et al. developed a full-scope simulator to evaluate the control and dynamic behavior of core parameters during Load-Following Operation (LFO). Their simulation involved a ±3% full power load change, based on various analyses and economic studies, leading to the recommendation of a specific deadband and coefficient [5]. Furthermore, other researchers have explored the impact of performing frequency operations on multi-unit small-size PWRs and its effect on the stability of the electricity grid. These studies highlight the significance of conducting LFO, particularly frequency operation, to improve the economy and stability of the electricity grid [6].

In this study, the applicability of Mode-K+ for performing secondary frequency operations will be discussed [7]. Mode-K was initially developed for Load-Following Operation (LFO) in the first generation of Korean nuclear power plants, KNGR, and it has since undergone several modifications to improve its performance and capabilities [8,9]. Mode-K+ will be introduced in the APR1400's initial cycle under various Burnup (BU) conditions and at different load change rates [10]. The analysis was conducted using the in-house diffusion-based code KANT, with two-group cross-sections generated by the SERPENT 2 Monte Carlo code and assessed with the ENDF/B-VII data library [11,12].

2. Reactor Description

The APR1400 is a PWR with a maximum rated thermal power of 3983 MWth. This analysis utilized the initial cycle of the APR1400, comprising 241 fresh fuel assemblies with varying enrichments (1.71, 2.64, 3.14, and 3.64 w/o). Figure 2 shows a quarter core configuration and fuel assemblies load pattern where A, B, and C refer to fuel assemblies with different enrichment. The reactor core includes three banks of Partial Strength Control Element Assemblies (PSCEA), which can operate independently or in any combination, and three Full Strength Control Element Assemblies (FSCEA) regulating banks (R5, R4, and R3) for use during LFO. Soluble boron is also employed for excess reactivity control, with the initial Critical Boron Concentration calculated using KANT at approximately 800 ppm after xenon equilibrium [13].

A0	A0	C3	A0	B1	A0	B3	C2	B0	1
A0	B3	A0	B3	A0	B1	A0	B3	C0	2
C3	A0	C2	A0	C3	A0	C3	B1	B0	3
A0	B3	A0	B3	A0	B3	A0	B2	C0	4
B1	A0	C3	A0	C2	A0	B1	C0		5
A0	B1	A0	B3	A0	B3	C1	C0		6
B3	A0	C3	A0	B1	C1	C0			7
C2	B3	B1	B2	C0	C0				8
B0	C0	B0	C0						9
A	B	C	D	E	F	G	H	I	

Figure 2 APR1400 initial core configuration and load pattern.

3. Computational Tool

Using KANT simulation tool, the time-dependent solution of the diffusion equation is performed using the NEM-CMFD acceleration module. The T/H coupling is also performed, where the temperature and moderator density derivative of the cross-sections are provided. While in this analysis, the U-Tube Steam Generator (UTSG) was also modeled for actual simulation of the inlet coolant temperature change. Figure 3 provides the flow diagram for the KANT simulation modules.

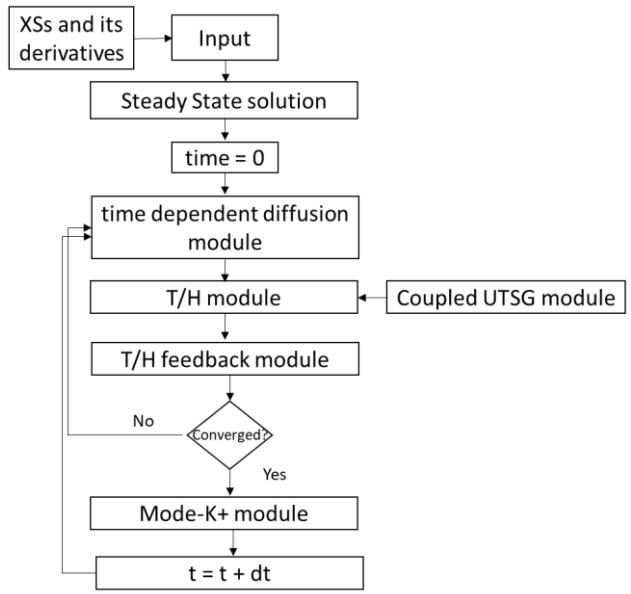

Figure 3 KANT simulation flow diagram.

4. Mode-K+ Control Logic

Mode-K+'s control logic operates based on the reactor core's physical behavior during Control Element Assembly (CEA) movements. Three signals are crucial for decision-making during operation. These are important to determine the reactivity status in the reactor core as well as the axial power distribution which is important to guarantee xenon stability. The first is the temperature mismatch (ΔT) between the target and measured average core coolant temperatures. Since the APR1400 operates with a fixed inlet coolant temperature, deviations in average and exit coolant temperatures as functions of reactor power are used to determine CEA movement direction. For example, a negative sign indicates a need for positive reactivity insertion to return to a critical state, and vice versa. The extent of deviation also influences the speed of CEA movement [7]. Figure 4 shows the temperature mismatch control signal. In this logic, the control action is initiated if ΔT exceeds T1, by moving the CEA at the minimum speed. If the temperature continues to increase and reaches the high-speed setpoint, the maximum speed will be selected to move the CEA. However, if ΔT is reduced to less than T1, the control flag will remain active unless ΔT is less than T1 by T2. This approach eliminates frequent switching of the control flag.

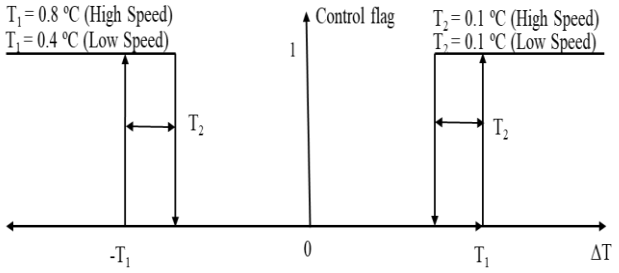

Figure 4 Mode-K+ temperature mismatch control signal setpoints.

The second important signal is the Axial-Shape Index (ASI), which measures axial power profile skewness. It is calculated as $\frac{P_B - P_T}{P_B + P_T}$ where PB is the bottom half power, and P_T is the top half power. It is assessed using ex-core axial detectors. Similar to ΔT, the deviation of ASI from a targetted value is measured. This target ASI value is usually determined via the unrodded depletion ASI value of the equilibrium core. The control flag will be determined if the ΔASI exceeds ±0.045 which is determined after multiple simulations to obtain acceptable behaviour. The physical concept dictates that a CEA movement in the core's bottom half will decrease the bottom half power, leading to a less positive ASI value. Conversely, withdrawal from the bottom half results in axial power shifting towards top-

skewness. The derivative of reactivity change to ASI change also relates to the CEA movement's location [7].

In some situations, the temperature mismatch may fall within the acceptable range. However, ASI control might still be necessary. In such cases, the direction for CEA selection will be based on the sign of ΔT, where a positive value indicates CEA insertion and a negative one signifies CEA withdrawal. Nevertheless, if no ASI-favorable CEA movement is possible in this direction, the control algorithm will seek preferred CEA movement in the opposite direction, provided that the temperature remains within the deadband. However, if no CEA can be selected in that direction to enhance the ASI, then no action will be taken.

The final signal is the core's boron concentration. Mode-K+ uses adjustments in soluble boron concentration to compensate for xenon reactivity changes. The decision on boron concentration is made by the reactor operator. This analysis assumes no boron adjustment during frequency operation due to minimal xenon concentration changes from fast and small power adjustments [14].

5. Results and Discussion

Figure 5 presents the power operation scenario considered in this study. Various power ramp-up and down speeds were analyzed, with the initial power set at 95%Pr to comply with limitations on operating nuclear power plants beyond their designed maximum rated power. The study implemented this scenario at both the Beginning of Cycle (BOC) with fresh core conditions and the End Of Cycle (EOC) with a higher BU condition. The primary differences between these conditions include the amount of soluble boron in the core and the neutron spectrum hardness at the EOC, leading to a more negative Moderator Temperature Coefficient (MTC).

Figure 6, illustrates the core parameters' status during secondary control at the BOC condition. It shows the initial insertion of PSCEAs 2 and 3 in the core, assuming the need for secondary frequency control during typical daily LFO. The simulation also highlights minor over and undershoots at the end of power ramp-up and ramp-down, respectively, due to the rapid CEA movement and the weak worth of the PSCEAs used. The initial Critical Boron Concentration was maintained throughout the simulation period, and ASI control remained within the ±0.27 design limit, with minimal change in value due to the use of weak PSCEA near the core's centerline. Inlet coolant temperature variations around the targeted value of 563 K occurred, but these were brief and returned to the nominal range quickly, posing no safety concerns as long as they adhered to allowable corrective action time limits.

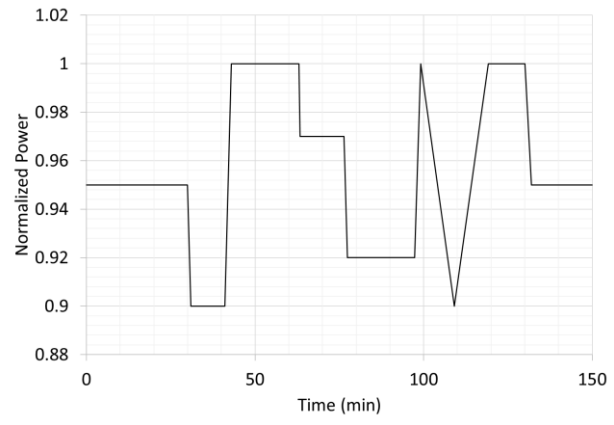

Figure 5 Secondary frequency operation simulation scenario.

Figure 7, displays similar core parameters at the EOC condition. Deeper CEA insertion, particularly of PSCEA 1, was necessary at the EOC due to the more negative MTC value requiring additional reactivity for temperature compensation. Power overshoots or undershoots at the EOC were slightly reduced because of the increased CEA worth. The CBC was maintained at its initial status without any boration or dilution, calculated at 164 ppm at the EOC. ASI variations were within acceptable limits, with maximum changes due to PSCEA-1 movement at the top of the core, affecting ASI significantly. The inlet coolant temperature showed less deviation from operation limits at the BOC due to smaller power overshoots or undershoots.

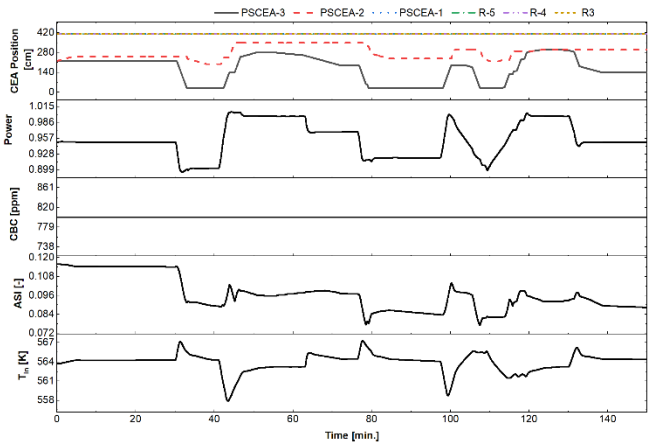

Figure 6 Secondary frequency operation in APR1400 at the BOC.

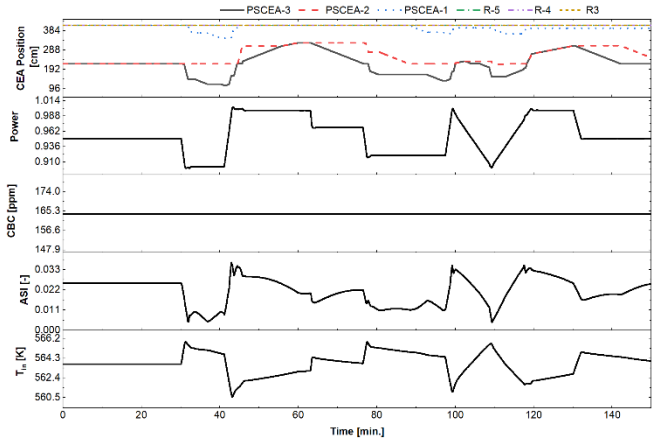

Figure 7 Secondary frequency operation in APR1400 at the EOC.

6. Conclusions and Future Work

The growing contribution of intermittent renewable sources highlights the increasing importance of frequency control to balance power demand and production. This study investigated the applicability of Mode-K+, developed for daily LFO in PWRs, for secondary frequency control in the APR1400. The analysis, conducted at the BOC and higher burnup conditions at the EOC, revealed a good match between targeted power scenarios and simulation results, with minimal overshoot or undershoot. The simulation assumed the initial insertion of PSCEA 2 and 3 up to the core's midplane, indicating the feasibility of frequency control during daily LFO. Future work will explore the potential for faster primary frequency control, even in different core configurations such as LEU+-loaded APR1400 cores.

ACKNOWLEDGMENT

This work was supported by the National Research Foundation of Korea (NRF) Grant funded by the Korean Government (MSIT) (RS-2022-00144429, and 2022M2E9A304619011).

REFERENCES

[1] Drudy, Keith J., Toshio Morita, and Barbara T. Connelley. "Robustness of the MSHIM Operation and Control Strategy in the AP1000 Design." In International Conference on Nuclear Engineering, vol. 43536, pp. 893-904. 2009.

[2] Lokhov, A., 2011. Technical and economic aspects of load following with nuclear power plants. NEA, OECD, Paris, France, 2.

[3] Abdelhameed, Ahmed Amin E., Jeongik Lee, and Yonghee Kim. "Physics conditions of passive autonomous frequency control operation in conventional large-size PWRs." Progress in Nuclear Energy 118 (2020): 103072.

[4] Abdelhameed, Ahmed Amin E., Xuan Ha Nguyen, Jeongik Lee, and Yonghee Kim. "Feasibility of passive autonomous frequency control operation in a Soluble-Boron-Free small PWR." Annals of Nuclear Energy 116 (2018): 319-333.

[5] Wang, Pengfei, Yan Fu, Xinyu Wei, and Fuyu Zhao. "Simulation study of frequency control characteristics of a generation III+ nuclear power plant." Annals of Nuclear Energy 115 (2018): 502-522.

[6] Sabir, Adeel, Dennis Michaelson, and Jin Jiang. "Load-frequency control with multimodule small modular reactor configuration: Modeling and dynamic analysis." IEEE Transactions on Nuclear Science 68, no. 7 (2021): 1367-1380.

[7] Khalefih, Husam, Yunseok Jeong, and Yonghee Kim. "Daily Load-Follow Operation in LEU+-Loaded APR1400 Using Mode-K+ Control Logic." International Journal of Energy Research 2023 (2023).

[8] Kim, Y. and Park, M., 2000. Evaluation of load-follow performance of Korean next-generation reactor (KNGR). PHYSOR, Pittsburgh.

[9] Oh, Soo-Youl, Jonghwa Chang, Jong-Kyun Park, and Manuel Carrasco. "Mode K—a core control logic for enhanced load-follow operations of a pressurized water reactor." Nuclear technology 134, no. 2 (2001): 196-207.

[10] Khalefih, Husam, and Yonghee Kim. "A Study on Control Algorithm for Daily Load-Follow Operation in the APR1400 Reactor." In American Nuclear Society Winter Meeting, vol. 127, pp. 1145-1148. 2022.

[11] Taesuk Oh, Yunseok Jeong, Husam Khalefih, Yonghee Kim, Development and validation of multiphysics PWR core simulator KANT, Nuclear Engineering and Technology, Volume 55, Issue 6,2023, Pages 2230-2245, ISSN 1738-5733.

[12] Leppänen, J., Pusa, M., Viitanen, T., Valtavirta, V. and Kaltiaisenaho, T., 2015. The Serpent Monte Carlo code: Status, development and applications in 2013. Annals of Nuclear Energy, 82, pp.142-150.

[13] U.S. Nuclear Regulatory Commission. "AP1000 Design Control Document: Chapter 4, Tier 2." Revision 19. PDF file: https://www.nrc.gov/docs/ML1117/ML11171A445.pdf.

[14] Khalefih, H., Jeong, Y. and Kim, Y., "A Study on Daily Load-follow Operation in the APR1400 Reactor using Manganese-Based Partial Strength Control Element Assembly," *Proc. Korea Nuclear Society*, Korea, Oct. 2022.